

GeoPro-VO: Dynamic Obstacle Avoidance with Geometric Projector Based on Velocity Obstacle

Jihao Huang¹, Xuemin Chi¹, Jun Zeng², Zhitao Liu^{1†}, Hongye Su¹

Abstract—Optimization-based approaches are widely employed to generate optimal robot motions while considering various constraints, such as robot dynamics, collision avoidance, and physical limitations. It is crucial to efficiently solve the optimization problems in practice, yet achieving rapid computations remains a great challenge for optimization-based approaches with nonlinear constraints. In this paper, we propose a geometric projector for dynamic obstacle avoidance based on velocity obstacle (GeoPro-VO) by leveraging the projection feature of the velocity cone set represented by VO. Furthermore, with the proposed GeoPro-VO and the augmented Lagrangian spectral projected gradient descent (ALSPG) algorithm, we transform an initial mixed integer nonlinear programming problem (MINLP) in the form of constrained model predictive control (MPC) into a sub-optimization problem and solve it efficiently. Numerical simulations are conducted to validate the fast computing speed of our approach and its capability for reliable dynamic obstacle avoidance.

I. INTRODUCTION

A. Motivation

Most robot motion planning tasks can be formulated as optimization problems, with various constraints like robot dynamics, safety and physical limitations [1]. Nonlinear model predictive control (NMPC) can consider all these constraints within a short prediction horizon and solve the constrained optimization problem in real time [2]. However, when the prediction horizon is long and non convex constraints are present, real time solution can not be guaranteed. In this paper, we propose to construct the geometric projector for dynamic obstacle avoidance based on velocity obstacle (GeoPro-VO) and integrate it with the augmented Lagrangian spectral projected gradient descent (ALSPG) algorithm to reformulate the nominal constrained NMPC problem into a sub-optimization problem for efficiently solving.

B. Related Works

1) *Projection-based Optimization Approaches*: In most optimization problems, constraints such as safety and physical limitations are typically described using geometric set primitives or combinations thereof. For instance, physical limitations are commonly modeled as box constraints. Safety

constraints, like avoiding collisions with ellipsoids or polytopes, are often expressed through quadratic sets, hyperplanes, and cone constraints. Some studies propose to leverage the projection feature of these sets instead of directly integrating them as geometric constraints in optimization problems. The projected gradient descent algorithm [3] is utilized to solve the sub-optimization problem of sequential quadratic programming (SQP) with faster efficiency than the second-order solver SNOPT [4]. Spectral projected gradient descent (SPG) [5] improves on the previous approach by utilizing curvature information through spectral step sizes. It has been applied across various fields for its great practical performance [6], outperforming even commercially available second-order solvers if a computationally efficient projection is used. However, using SPG alone can only solve optimization problems with physical constraints on the control's boundaries, it is not sufficient to solve optimization problems in robotics with complex nonlinear constraints, such as collision avoidance constraints.

In addition, some studies [7]–[10] integrate SPG with the augmented Lagrangian framework to overcome the limitations of SPG, and this algorithm is commonly referred to as augmented Lagrangian spectral projected gradient descent (ALSPG). ALSPG first incorporates the constraint violation size as a cost function into the objective function of the nominal optimization problem, resulting in a sub-optimization problem only with physical constraints on control boundaries. In addition, the sub-optimization problem is solved by SPG efficiently. To effectively reformulate the nominal optimization problem with the augmented Lagrangian framework, a more general framework based on the concept of geometric projector (GeoPro) is proposed in [11]. GeoPro can effectively project a point onto a set, enabling us to quickly calculate the magnitude of constraint violations. Chi *et al.* [11] briefly describes collision avoidance constraints using GeoPro as follows: if the current state is within the set of obstacle, GeoPro will efficiently project the state to the set's boundary; otherwise, it will maintain the current state. However, [11] mainly constructs GeoPro for collision avoidance based on the Euclidean distance and projects the unsafe robot positions to the boundary of obstacles, which may not perform well with dynamic obstacles.

2) *Velocity Obstacle*: Collision cone [12] is a commonly crucial concept for local and reactive collision avoidance, and velocity obstacle (VO) is indeed a specific type of collision cone. VO and its variants [13]–[16] have been widely employed to realize collision avoidance and navigation with both static and dynamic obstacles for robots. VO

This work was supported in part by National Key R&D Program of China (Grant NO. 2021YFB3301000); National Natural Science Foundation of China (NSFC:62173297), Zhejiang Key R&D Program (Grant NO. 2022C01035).

¹Jihao Huang, Xuemin Chi, Zhitao Liu and Hongye Su are with the State Key Laboratory of Industrial Control Technology, Institute of Cyber-Systems and Control, Zhejiang University, Hangzhou, China {jihao, chixuemin, ztliu, hysu}@zju.edu.cn. ²Jun Zeng is with Cruise LLC, USA jun.zeng@getcruise.com.

[†] Corresponding author.

is defined as the set of all velocities for a robot which will lead to a collision with an obstacle at some future moment, with the assumption that the obstacle maintains its current velocity. By choosing a velocity outside of VO induced by the obstacle, collision avoidance is guaranteed between them. In addition, the robot can select a velocity which is outside of any VO induced by all obstacles to avoid collisions with all obstacles. Since VO explicitly considers the velocity of the obstacle and described the sets of unsafe velocity, making it suitable for dynamic obstacle avoidance. In addition, in order to design dynamic collision avoidance controllers for the robot controlled by acceleration, some studies [17], [18] formulate collision avoidance constraints based on VO or its variants. Zhang *et al.* [18] propose integrating VO with the nonlinear model predictive control (NMPC), and formulate the obstacle avoidance constraint for velocity outside of VO as the velocity should be within the union of two half spaces. Since the condition that the velocity is within the union of two half spaces cannot be represented directly in terms of one single constraint, it is represented as a form in which at least one of two individual constraints is required to be met (each constraint requires the velocity within a half space). With such constraints, the nominal constrained NMPC problem introduces integer variables and becomes a mixed integer nonlinear programming problem (MINLP) [19], which requires a lot of time to solve. However, the velocity set represented by VO is a cone with good projection feature that can be integrated with GeoPro. Therefore, we aim to construct GeoPro for dynamic obstacle avoidance based on VO as follows: if the robot's velocity is within VO, project it to the boundary of VO; otherwise, maintain it. With the introduction of GeoPro, the solution of the initial MINLP can be avoided and the overall solution efficiency can be improved.

C. Contributions

In this paper, we propose to construct GeoPro for dynamic obstacle avoidance based on VO (GeoPro-VO) and solve the initial optimization problem with GeoPro-VO and ALSPG efficiently. The key contributions are as follows:

- We leverage the projection feature of the velocity cone set represented by VO to construct GeoPro-VO, which projects the unsafe velocity inside the VO outside the VO to achieve dynamic obstacle avoidance.
- By combining GeoPro-VO and the ALSPG algorithm, the nominal MINLP in the form of constrained NMPC is reformulated as a sub-optimization problem only with the physical constraints on controls, which can be solved by SPG with computational efficiency.
- Extensive numerical simulations have been conducted to validate that our approach can efficiently solve the sub-optimization problem and improve navigation safety. With proposed approach, the robot is able to reach its destination while avoiding collisions with both static and dynamic obstacles, even when the prediction horizon of MPC is short.

D. Organization

The rest of this paper are organized as follows: we formally define the nominal constrained NMPC optimization problem, review the concept of GeoPro and VO in Sec. II. In Sec. III, we introduce how to construct GeoPro-VO and integrate it with the ALSPG algorithm. The effectiveness and performance of our approach are demonstrated in Sec. IV. Sec. V concludes the paper.

II. PROBLEM DEFINITION & PRELIMINARIES

A. Problem Definition

Assume there is a robot with multiple obstacles in the environment. The robot's dynamics follow the double integral model:

$$\dot{x} = v_x, \dot{y} = v_y, \dot{v}_x = a_x, \dot{v}_y = a_y, \quad (1)$$

where the robot states are $\mathbf{x} = [x, y, v_x, v_y]^T$ with controls $\mathbf{u} = [a_x, a_y]^T$. The obstacle dynamics are similar to those of the robot with states $\mathbf{x}_{o_i} = [x_o, y_o, v_{ox}, v_{oy}]^T$. The positions and velocities of the robot and obstacle are represented by $\mathbf{p}_R = [x, y]^T$, $\mathbf{p}_{o_i} = [x_o, y_o]^T$, $\mathbf{v}_R = [v_x, v_y]^T$ and $\mathbf{v}_{o_i} = [v_{ox}, v_{oy}]^T$. Let $\mathbf{p}_R^{o_i} := \mathbf{p}_R - \mathbf{p}_{o_i}$ and $\mathbf{v}_R^{o_i} := \mathbf{v}_R - \mathbf{v}_{o_i}$ be the relative position and velocity between R and o_i . Both robot and obstacles are assumed to be circular-shaped with radii r and r_o , respectively.

Our work focuses on navigating a robot to its destination while avoiding collisions with all obstacles. The entire problem is formulated as a constrained nonlinear model predictive control (NMPC) optimization problem:

NMPC:

$$\min_{\mathcal{X}, \mathcal{U}} l(\mathcal{X}, \mathcal{U}) = \sum_{k=0}^{N-1} h(\mathbf{x}_k, \mathbf{u}_k) \quad (2a)$$

$$\text{s.t. } \mathbf{x}_{k+1} = f(\mathbf{x}_k, \mathbf{u}_k), \quad (2b)$$

$$\mathbf{g}_i(\mathbf{x}_k) \in \mathcal{C}_i, \forall i = 1, 2, \dots, N_p, \quad (2c)$$

$$\mathbf{x} \in \mathcal{D}_x, \quad (2d)$$

$$\mathbf{u} \in \mathcal{D}_u, \quad (2e)$$

where $\mathcal{X} = [\mathbf{x}_1^T, \dots, \mathbf{x}_N^T]^T \in \mathbb{R}^{N \cdot n_x}$, N is the predict horizon of NMPC, $\mathcal{U} = [\mathbf{u}_0^T, \dots, \mathbf{u}_{N-1}^T]^T \in \mathbb{R}^{N \cdot n_u}$ and N_p is the number of safety constraints. $h : \mathbb{R}^{n_x} \times \mathbb{R}^{n_u} \rightarrow \mathbb{R}$ is the cost function which depends on the robot's task, such as navigating robot to the goal position or minimizing controls. The system dynamics $f : \mathbb{R}^{n_x} \times \mathbb{R}^{n_u} \rightarrow \mathbb{R}^{n_x}$ are same to (1). $\mathbf{g}_i(\mathbf{x}_k) \in \mathcal{C}_i$ means the robot should within the security zone, where $\mathbf{g}_i : \mathbb{R}^{n_x} \rightarrow \mathbb{R}^{n_i}$, $\mathcal{C}_i \in \mathbb{R}^{n_i}$. Constraints (2d) and (2e) represent the physical limitations on states and controls respectively, indicating that both states and controls should fall within a reasonable range.

B. Geometric Projector

Geometric projector (GeoPro) [11] is proposed to project geometric constraints and then reformulated the nominal optimization problem to a sub-optimization problem with

the augmented Lagrangian method. Taking the nominal constrained NMPC problem (2) as an example ((2d) is omitted here for brevity), it can be reformulated with the classic augmented Lagrangian approach as

$$\mathcal{L}(\mathcal{X}, \mathcal{U}, \boldsymbol{\lambda}, \boldsymbol{\rho}) := l(\mathcal{X}, \mathcal{U}) + \sum_{i=1}^{N_p} \frac{\rho_{C_i}}{2} d_{C_i}^2(\mathbf{g}_i(\mathcal{X}) + \frac{\boldsymbol{\lambda}_{C_i}}{\rho_{C_i}}),$$

where $\boldsymbol{\lambda} = [\boldsymbol{\lambda}_{C_1}, \dots, \boldsymbol{\lambda}_{C_{N_p}}]^T$, $\boldsymbol{\lambda}_{C_i} \in \mathbb{R}^{n_i}$ is the Lagrangian multipliers, $\boldsymbol{\rho} = [\rho_{C_1}, \dots, \rho_{C_{N_p}}]^T$, $\rho_{C_i} \in \mathbb{R}$ is the penalty parameters and $d_{C_i}^2(\mathbf{y}_0) = \min_{\mathbf{y}} \|\mathbf{y} - \mathbf{y}_0\|$, $\mathbf{y} \in C_i$, which means the minimum distance from \mathbf{y}_0 to the set C_i . GeoPro is defined as $\mathcal{P}_{C_i}(\mathbf{y}_0) = \arg \min_{\mathbf{y} \in C_i} \|\mathbf{y} - \mathbf{y}_0\|$.

In addition, we can use the GeoPro \mathcal{P}_{C_i} to obtain the following compact form:

$$\mathcal{L}(\mathcal{X}, \mathcal{U}, \boldsymbol{\lambda}, \boldsymbol{\rho}) := l(\mathcal{X}, \mathcal{U}) + \sum_{i=1}^{N_p} \frac{\rho_{C_i}}{2} \left\| \mathbf{g}_i(\mathcal{X}) + \frac{\boldsymbol{\lambda}_{C_i}}{\rho_{C_i}} - \mathcal{P}_{C_i}(\mathbf{g}_i(\mathcal{X}) + \frac{\boldsymbol{\lambda}_{C_i}}{\rho_{C_i}}) \right\|^2, \quad (3)$$

where the level of constraints illegality are incorporated into the objective function as additional costs through GeoPro. If $\mathbf{g}_i(\mathbf{x}_k) \in C_i$, no additional cost is incurred in (3) since $\mathcal{P}_{C_i}(\mathbf{g}_i(\mathbf{x}_k)) = \mathbf{g}_i(\mathbf{x}_k)$ retains the original state. Conversely, if $\mathbf{g}_i(\mathbf{x}_k) \notin C_i$, we need to project $\mathbf{g}_i(\mathbf{x}_k)$ with GeoPro onto the surface of C_i with additional cost in (3). Using obstacle avoidance constraints as examples, as both the robot and obstacles are in circular-shaped, we can establish obstacle avoidance constraints using the Euclidean distance as follows:

$$\|\mathbf{p}_R^{\mathbf{o}_i}\|_2 \geq r + r_{\mathbf{o}_i}. \quad (4)$$

In addition, we can construct the GeoPro based on the constraint (4) mentioned above, referred to as GeoPro-ED:

$$\mathcal{P}_{ED_i}(\mathbf{p}_R) = \begin{cases} \mathbf{p}_R, & \|\mathbf{p}_R^{\mathbf{o}_i}\|_2 \geq r + r_{\mathbf{o}_i} \\ \mathbf{p}_R + \frac{\mathbf{p}_R^{\mathbf{o}_i}(r + r_{\mathbf{o}_i} - \|\mathbf{p}_R^{\mathbf{o}_i}\|_2)}{\|\mathbf{p}_R^{\mathbf{o}_i}\|_2}, & \|\mathbf{p}_R^{\mathbf{o}_i}\|_2 < r + r_{\mathbf{o}_i} \end{cases}. \quad (5)$$

Furthermore, GeoPro can also consider box constraints like (2d) to restrict the robot's states. To conclusion, GeoPro plays a significant role when constraints are violated.

C. Velocity Obstacle

The subscript k of time notation is dropped for simplicity. Let there be a robot R and an obstacle \mathbf{o}_i with radii r and $r_{\mathbf{o}_i}$. The velocity obstacle (VO) for R induced by \mathbf{o}_i is denoted as $\text{VO}_R^{\mathbf{o}_i}(\mathbf{v}_{\mathbf{o}_i})$, which includes all velocities of R that would lead to a collision between R and \mathbf{o}_i at future time moment, with assumption that \mathbf{o}_i moves with the constant velocity $\mathbf{v}_{\mathbf{o}_i}$.

Before introducing VO, let $A \oplus B = \{a+b | a \in A, b \in B\}$ be the Minkowski sum of sets A and B , and $\lambda(\mathbf{p}, \mathbf{v}) = \{\mathbf{p} + t\mathbf{v} | t > 0\}$ denotes a ray starting at point \mathbf{p} and in the direction of vector \mathbf{v} . If a ray starting at \mathbf{p}_R and heading in the direction of the relative velocity $\mathbf{v}_R - \mathbf{v}_{\mathbf{o}_i}$ intersects the Minkowski sum of \mathbf{o}_i and $-\mathbf{R}$ centered at $\mathbf{p}_{\mathbf{o}_i}$, then $\mathbf{v}_R \in \text{VO}_R^{\mathbf{o}_i}(\mathbf{v}_{\mathbf{o}_i})$. Hence, $\text{VO}_R^{\mathbf{o}_i}(\mathbf{v}_{\mathbf{o}_i})$ is defined as follows [13]:

$$\text{VO}_R^{\mathbf{o}_i}(\mathbf{v}_{\mathbf{o}_i}) = \{\mathbf{v}_R | \lambda(\mathbf{p}_R, \mathbf{v}_R - \mathbf{v}_{\mathbf{o}_i}) \cap \mathbf{o}_i \oplus -\mathbf{R} \neq \emptyset\}.$$

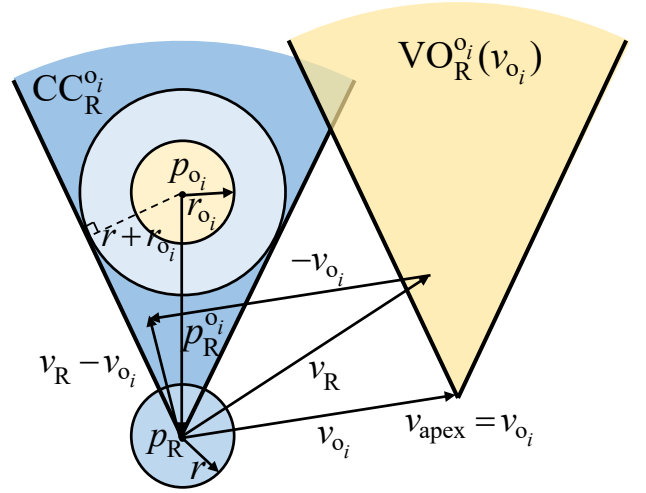


Fig. 1: Velocity obstacle $\text{VO}_R^{\mathbf{o}_i}(\mathbf{v}_{\mathbf{o}_i})$ of robot R induced by the obstacle \mathbf{o}_i . $\text{CC}_R^{\mathbf{o}_i}$ denotes the collision cone between them. If the relative velocity $\mathbf{v}_R - \mathbf{v}_{\mathbf{o}_i} \in \text{CC}_R^{\mathbf{o}_i}$ or the robot velocity $\mathbf{v}_R \in \text{VO}_R^{\mathbf{o}_i}(\mathbf{v}_{\mathbf{o}_i})$, a collision will occur between R and \mathbf{o}_i .

Therefore, if $\mathbf{v}_R \in \text{VO}_R^{\mathbf{o}_i}(\mathbf{v}_{\mathbf{o}_i})$, R and \mathbf{o}_i will collide at some future moment. On the contrary, if $\mathbf{v}_R \notin \text{VO}_R^{\mathbf{o}_i}(\mathbf{v}_{\mathbf{o}_i})$, R and \mathbf{o}_i will never collide. In fact, $\text{VO}_R^{\mathbf{o}_i}(\mathbf{v}_{\mathbf{o}_i})$ is a cone with its apex at $\mathbf{v}_{\mathbf{o}_i}$, as shown in Fig. 1, and it can be translated from the collision cone (CC) defined as follows:

$$\text{CC}_R^{\mathbf{o}_i} = \{\mathbf{v}_R - \mathbf{v}_{\mathbf{o}_i} | \lambda(\mathbf{p}_R, \mathbf{v}_R - \mathbf{v}_{\mathbf{o}_i}) \cap \mathbf{o}_i \oplus -\mathbf{R} \neq \emptyset\}.$$

In addition, $\text{VO}_R^{\mathbf{o}_i}(\mathbf{v}_{\mathbf{o}_i}) = \text{CC}_R^{\mathbf{o}_i} \oplus \mathbf{v}_{\mathbf{o}_i}$, the only distinction between these two cones lies in their apex positions: $\text{CC}_R^{\mathbf{o}_i}$ is at $\mathbf{0}$ as it considers relative velocity.

VO is commonly utilized for enabling robot to avoid collisions with obstacles by choosing a velocity that lies outside any of the VO induced by each obstacle. Many works have been proposed to address the limitations of VO in effectively avoiding collisions between multiple robots, such as reciprocal velocity obstacle (RVO) [14], hybrid reciprocal velocity obstacle (HRVO) [16] and optimal reciprocal collision avoidance (ORCA) [15]. Since VO defines the cone set of velocity, we aim to take full advantage of the projection properties of the cone set to construct GeoPro, more details can refer to Sec. III-A.

III. METHOD DESIGN

In this section, we will first demonstrate how to build the GeoPro for dynamic obstacle avoidance based on VO (GeoPro-VO) in the velocity space. Additionally, we will discuss integrating the GeoPro-VO into ALSPG and provide a more detailed overview of the algorithmic steps involved in ALSPG.

A. Geometric Projector Based on Velocity Obstacle

In this section, we mainly introduce how to construct the GeoPro-VO based on the robot dynamics (1). For the robot dynamics without horizontal and vertical velocity v_x and v_y , we can use the differentiation of horizontal position and

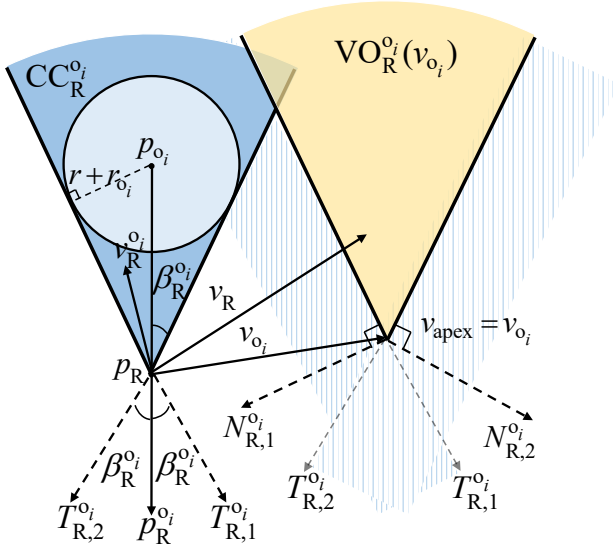


Fig. 2: Constructing the hyperplanes for $\text{VO}_R^{o_i}(v_{o_i})$. R can avoid collisions with o_i if $\bigcup_{m \in \{1,2\}} (N_{R,m}^{o_i})^T v_R \geq c_{R,m}^{o_i}$, which means $v_R \notin \text{VO}_R^{o_i}(v_{o_i})$.

vertical position with respect to time to represent v_x and v_y . Taking the bicycle model as an example:

$$v_x = \dot{x} = v \cos \theta, v_y = \dot{y} = v \sin \theta.$$

In the following, we will demonstrate how to leverage the project feature of the cone set to construct GeoPro-VO.

As we mentioned above, the robot R will avoid collisions with the obstacle o_i when $v_R \notin \text{VO}_R^{o_i}(v_{o_i})$. The two tangent vectors $T_{R,1}^{o_i}$ and $T_{R,2}^{o_i}$ of $\text{CC}_R^{o_i}$ shown in Fig. 2 can be computed as

$$T_{R,1}^{o_i} = R(\beta_R^{o_i})p_R^{o_i}, T_{R,2}^{o_i} = R(-\beta_R^{o_i})p_R^{o_i},$$

where

$$R(\beta) = \begin{bmatrix} \cos \beta & -\sin \beta \\ \sin \beta & \cos \beta \end{bmatrix}.$$

Furthermore, the normal vectors of these two tangent vectors can be obtained by rotating them like

$$N_{R,1}^{o_i} = R(-\frac{\pi}{2})T_{R,1}^{o_i}, N_{R,2}^{o_i} = R(\frac{\pi}{2})T_{R,2}^{o_i}.$$

Since VO is translated form CC, the normal and tangent vectors of VO are the same as these of CC, as shown in Fig. 2. With the property $\text{VO}_R^{o_i}(0) = \text{CC}_R^{o_i}$, we can derive if $v_R \notin \text{CC}_R^{o_i}$, collision avoidance is achieved. This condition can be represented by the following two linear constraints:

$$v_R \notin \text{CC}_R^{o_i} \iff \bigcup_{m \in \{1,2\}} (N_{R,m}^{o_i})^T v_R \geq 0, \quad (6)$$

which means we can represent the safe region of $v_R^{o_i}$ by using the union of two half spaces. In addition, we reformulate condition (6) with the absolute velocity as

$$v_R \notin \text{VO}_R^{o_i}(v_{o_i}) \iff \bigcup_{m \in \{1,2\}} (N_{R,m}^{o_i})^T v_R \geq c_{R,m}^{o_i}, \quad (7)$$

where $c_{R,m}^{o_i} = (N_{R,m}^{o_i})^T v_{o_i}$ is the scalar corresponding to the m^{th} linear constraint of $v_R \notin \text{VO}_R^{o_i}(v_{o_i})$. Condition (7) is precisely the obstacle avoidance constraint based on VO. However, when we attempt to directly incorporate (7) into (2), integer variables are required to ensure that at least one of these two constraints is required to be met. The detailed form of VO-based NMPC (VO-NMPC) is as follows:

VO-NMPC:

$$\begin{aligned} \min_{\mathcal{X}, \mathcal{U}} l(\mathcal{X}, \mathcal{U}) &= \sum_{k=0}^{N-1} h(x_k, u_k) \\ \text{s.t. } (2b), (2d), (2e), \\ c_{R,m}^{o_i} - (N_{R,m}^{o_i})^T v_R &\leq G(1 - z_{i,m}), \\ i &= 1, 2, \dots, N_p, m = 1, 2, \end{aligned} \quad (8a)$$

$$\sum_{m=1}^2 z_{i,m} \geq 1, z_{i,m} \in \{0, 1\}. \quad (8b)$$

where $z_{i,m}$ is the integer variable and G is a large positive real number, such as 10^5 . The subscripts k for time notation of (8a) and (8b) are also dropped for brevity. The nominal optimization problem (2) is transformed into a mixed integer nonlinear programming problem (MINLP). Solving MINLP requires a large amount of computation time, making it unsuitable for real time applications.

In our work, we aim to address the aforementioned issues using GeoPro-VO and ALSPG. If $v_R \notin \text{VO}_R^{o_i}(v_{o_i})$, GeoPro-VO will maintain the original state as the velocity is within the safe range, i.e., $\mathcal{P}_{\text{VO}_i}(v_R) = v_R$, where $\mathcal{P}_{\text{VO}_i}$ also falls under \mathcal{P}_{C_i} . Moreover, if $v_R \in \text{VO}_R^{o_i}(v_{o_i})$, which can be represented using the two linear constraints as:

$$v_R \in \text{VO}_R^{o_i}(v_{o_i}) \iff \bigcap_{m \in \{1,2\}} (N_{R,m}^{o_i})^T v_R \leq c_{R,m}^{o_i}. \quad (9)$$

Rewriting condition (9) to a matrix form as

$$\begin{aligned} v_R \in \text{VO}_R^{o_i}(v_{o_i}) &\iff v_R \in \mathcal{C}_i^{\text{VO}} := \{v \in \mathbb{R}^2 : Av \leq b\}, \\ A &= \begin{bmatrix} (N_{R,1}^{o_i})^T \\ (N_{R,2}^{o_i})^T \end{bmatrix} \in \mathbb{R}^{2 \times 2}, b = \begin{bmatrix} c_{R,1}^{o_i} \\ c_{R,2}^{o_i} \end{bmatrix} \in \mathbb{R}^2. \end{aligned}$$

In this scenario, we need to project v_R onto the nearest hyperplane with respect to A and b for safety, as shown in Fig. 3. Then the GeoPro-VO can be described by

$$\mathcal{P}_{\text{VO}_i}(v_R) = v_R - \frac{a(a^T v_R - b)}{\|a\|_2},$$

where $a^T x = b$ represents the closest hyperplane for projecting v_R w.r.t A and b .

In conclusion, with our proposed GeoPro-VO, we can project the unsafe velocity into the safe range to achieve dynamic obstacle avoidance between robot and obstacles. In addition, physical limitations of states such as $v_x^{\min} \leq v_x \leq v_x^{\max}$ and $v_y^{\min} \leq v_y \leq v_y^{\max}$ can also be described by GeoPro, as

$$\mathcal{P}_{\mathcal{D}_x}(v_R) = \begin{cases} v_R, v^{\min} \preceq v_R \preceq v^{\max} \\ v^{\min}, v_R \preceq v^{\min} \\ v^{\max}, v^{\max} \preceq v_R \end{cases}. \quad (10)$$

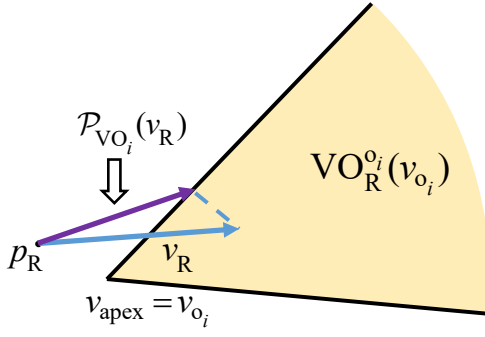


Fig. 3: If $v_R \in VO_R^o(v_{o_i})$, project the unsafe velocity to the nearest hyperplane.

By combining the proposed \mathcal{P}_{VO_i} and $\mathcal{P}_{\mathcal{D}_x}$ with the augmented Lagrangian framework, we can reformulate (8) into the form like (3). Physical limitations of controls are considered in solving (3) through spectral projected gradient descent (SPG), more details please refer to Sec. III-B. We need to mention through leveraging the projection feature of VO to construct GeoPro, we can eliminate integer variables in (8a) and obtain real time solutions for practical applications.

B. Augmented Lagrangian Spectral Projected Gradient Descent (ALSPG)

Since SPG by itself is inadequate for tackling robotics problems with complex nonlinear constraints, ALSPG is proposed as a solution to this issue. Using the augmented Lagrangian framework, (2) is reformulated as (3). It should be noted that (2d) is excluded in (3) for brevity; however, the physical limitations of states should also be included in (3) in practice. For convenience of updating the penalty parameters, we define a distance function as follows:

$$V_{c_i}(\mathcal{X}, \lambda_{c_i}, \rho_{c_i}) := g_i(\mathcal{X}) - \mathcal{P}_{c_i}(g_i(\mathcal{X}) + \frac{\lambda_{c_i}}{\rho_{c_i}}). \quad (11)$$

Furthermore, let $V := [V_{c_1}^T, V_{c_2}^T, \dots, V_{c_{N_p}}^T]^T \in \mathbb{R}^{\sum_{i=1}^{N_p} n_i}$. The norm of V can be utilized to design a termination criterion of ALSPG, when $\|V\| \leq \varepsilon_{\text{tol}}$, $\varepsilon_{\text{tol}} > 0$, iterations of ALSPG will terminate. Since (2) includes an additional system constraint (2b), we reformulate (3) by eliminating the variable \mathcal{X} using (2b). First, through the standard linearization of the system dynamics (2b), we can derive that

$$A_k = \frac{\partial f(x_k, u_k)}{\partial x_k}, B_k = \frac{\partial f(x_k, u_k)}{\partial u_k},$$

where $A_k \in \mathbb{R}^{n_x \times n_x}$ and $B_k \in \mathbb{R}^{n_x \times n_u}$. Moreover, the system dynamics integration is represented as $\mathcal{X} = \mathcal{A}x_0 + \mathcal{B}U$:

$$\mathcal{A} = \begin{bmatrix} A_0 \\ A_1 A_0 \\ \vdots \\ \prod_{i=0}^{N-2} A_i \\ \prod_{i=0}^{N-1} A_i \end{bmatrix}, \mathcal{B} = \begin{bmatrix} B_0 & 0 & \dots & 0 & 0 \\ A_1 B_0 & B_1 & \dots & 0 & 0 \\ \vdots & \vdots & \ddots & \vdots & \vdots \\ \prod_{i=0}^{N-2} A_i B_0 & \prod_{i=0}^{N-2} A_i B_1 & \dots & B_{N-2} & 0 \\ \prod_{i=0}^{N-1} A_i B_0 & \prod_{i=0}^{N-1} A_i B_1 & \dots & A_{N-1} B_{N-2} & B_{N-1} \end{bmatrix}.$$

where $\mathcal{A} \in \mathbb{R}^{(N \cdot n_x) \times n_x}$, $\mathcal{B} \in \mathbb{R}^{(N \cdot n_x) \times (N \cdot n_u)}$ and x_0 is the initial state of the robot at time step 0. Let $\phi(\mathcal{U}) := \{\mathcal{X} \in \mathbb{R}^{N \cdot n_x} : \mathcal{A}x_0 + \mathcal{B}U\}$. In addition, the cost function of (2)

can be rewritten as $l(\mathcal{X}, \mathcal{U}) := l(\phi(\mathcal{U}), \mathcal{U}) = l(\mathcal{U})$. With the above equations, (3) is simplified to

$$\mathcal{L}(\mathcal{U}, \lambda, \rho) := l(\mathcal{U}) + \sum_{i=1}^{N_p} \frac{\rho_{c_i}}{2} \|g_i(\mathcal{U}) + \frac{\lambda_{c_i}}{\rho_{c_i}} - \mathcal{P}_{c_i}(g_i(\mathcal{U}) + \frac{\lambda_{c_i}}{\rho_{c_i}})\|^2. \quad (12)$$

And (11) is also simplified to:

$$V_{c_i}(\mathcal{U}, \lambda_{c_i}, \rho_{c_i}) := g_i(\mathcal{U}) - \mathcal{P}_{c_i}(g_i(\mathcal{U}) + \frac{\lambda_{c_i}}{\rho_{c_i}}).$$

The Jacobi matrices of the cost function $l(\mathcal{U})$ w.r.t \mathcal{X} and \mathcal{U} are represented by $J_{\mathcal{X}} = \frac{\partial l(\mathcal{X}, \mathcal{U})}{\partial \mathcal{X}} \in \mathbb{R}^{N \cdot n_x}$ and $J_{\mathcal{U}} = \frac{\partial l(\mathcal{X}, \mathcal{U})}{\partial \mathcal{U}} \in \mathbb{R}^{N \cdot n_u}$. Thus the partial derivatives of $l(\mathcal{U})$ and $g_i(\mathcal{U})$ w.r.t \mathcal{U} are:

$$\begin{aligned} \nabla l(\mathcal{U}) &= \frac{\partial l(\mathcal{U})}{\partial \mathcal{U}} + \frac{\partial \phi(\mathcal{U})}{\partial \mathcal{U}} \frac{\partial l(\phi(\mathcal{U}))}{\partial \phi(\mathcal{U})} = J_{\mathcal{U}} + \mathcal{B}^T J_{\mathcal{X}} \\ \frac{\partial g_i(\mathcal{U})}{\partial \mathcal{U}} &= \frac{\partial \phi(\mathcal{U})}{\partial \mathcal{U}} \frac{\partial g_i(\phi(\mathcal{U}))}{\partial \phi(\mathcal{U})} = \mathcal{B}^T \nabla g_i \end{aligned}$$

where $\nabla g_i = \frac{\partial g_i(\mathcal{X})}{\partial \mathcal{X}} \in \mathbb{R}^{N \cdot n_x \times n_i}$. Moreover, the derivative of (12) with respect to time is:

$$\begin{aligned} \nabla \mathcal{L}(\mathcal{U}, \lambda, \rho) &= \nabla l(\mathcal{U}) + \sum_{i=1}^{N_p} \rho_{c_i} \frac{\partial g_i(\mathcal{U})}{\partial \mathcal{U}} (V_{c_i} + \frac{\lambda_{c_i}}{\rho_{c_i}}) \\ &= \mathcal{B}^T J_{\mathcal{X}} + J_{\mathcal{U}} + \sum_{i=1}^{N_p} \rho_{c_i} \mathcal{B}^T \nabla g_i (V_{c_i} + \frac{\lambda_{c_i}}{\rho_{c_i}}) \\ &= \mathcal{B}^T (J_{\mathcal{X}} + \nabla \mathcal{G} \Lambda \mathcal{V}) + J_{\mathcal{U}}, \end{aligned} \quad (13)$$

where

$$\begin{aligned} \nabla \mathcal{G} &= \begin{bmatrix} \nabla g_1 & \nabla g_2 & \dots & \nabla g_{N_p} \end{bmatrix} \in \mathbb{R}^{N \cdot n_x \times \sum_{i=1}^{N_p} n_i} \\ \Lambda &= \begin{bmatrix} \rho_{c_1} I & & & \\ & \rho_{c_2} I & & \\ & & \ddots & \\ & & & \rho_{c_{N_p}} I \end{bmatrix} \in \mathbb{R}^{\sum_{i=1}^{N_p} n_i \times \sum_{i=1}^{N_p} n_i} \\ \rho_{c_i} I &= \begin{bmatrix} \rho_{c_i} & 0 & \dots & 0 \\ 0 & \rho_{c_i} & \dots & 0 \\ \vdots & \vdots & \ddots & \vdots \\ 0 & 0 & \dots & \rho_{c_i} \end{bmatrix} \in \mathbb{R}^{n_i \times n_i}, \\ \mathcal{V} &= \begin{bmatrix} V_{c_1} + \frac{\lambda_{c_1}}{\rho_{c_1}} \\ V_{c_2} + \frac{\lambda_{c_2}}{\rho_{c_2}} \\ \vdots \\ V_{c_{N_p}} + \frac{\lambda_{c_{N_p}}}{\rho_{c_{N_p}}} \end{bmatrix} \in \mathbb{R}^{\sum_{i=1}^{N_p} n_i} \end{aligned}$$

To efficiently compute (13), we use a recursive iteration approach. Let $\omega = [\omega_0^T, \omega_1^T, \dots, \omega_{N-1}^T]^T \in \mathbb{R}^{N \cdot n_x}$ be the vector to multiply, and $z = [z_0^T, z_1^T, \dots, z_{N-1}^T]^T \in \mathbb{R}^{N \cdot n_u}$ be the resulting vector. Then we have $z = \mathcal{B}^T \omega$:

$$\begin{bmatrix} z_0 \\ z_1 \\ \vdots \\ z_{N-2} \\ z_{N-1} \end{bmatrix} = \begin{bmatrix} B_0^T & B_0^T A_1^T & \dots & B_0^T \prod_{i=1}^{N-2} A_i^T & B_0^T \prod_{i=1}^{N-1} A_i^T \\ 0 & B_1^T & \dots & B_1^T \prod_{i=2}^{N-2} A_i^T & B_1^T \prod_{i=2}^{N-1} A_i^T \\ \vdots & \vdots & \ddots & \vdots & \vdots \\ 0 & 0 & \dots & B_{N-2}^T & B_{N-2}^T A_{N-1}^T \\ 0 & 0 & \dots & 0 & B_{N-1}^T \end{bmatrix} \begin{bmatrix} \omega_0 \\ \omega_1 \\ \vdots \\ \omega_{N-2} \\ \omega_{N-1} \end{bmatrix}.$$

In addition, we have the following recursive equations in a reverse order:

$$\begin{aligned} \mathbf{z}_k &= B_k^T \tilde{\mathbf{z}}_k, \\ \tilde{\mathbf{z}}_k &= \boldsymbol{\omega}_k + A_{k+1}^T \tilde{\mathbf{z}}_{k+1}, \\ \tilde{\mathbf{z}}_{N-1} &= \mathbf{w}_{N-1}. \end{aligned}$$

To conclusion, with the augmented Lagrangian framework we have reformulated (2) as a constrained and non-convex problem:

$$\arg \min_{\mathcal{U} \in \mathcal{D}_u} \mathcal{L}(\mathcal{U}, \boldsymbol{\lambda}, \boldsymbol{\rho}). \quad (14)$$

Moreover, we can solve this sub optimization-problem (14) using SPG with the geometric projector $\mathcal{P}_{\mathcal{D}_u}$ that is similar to (10). For more details about SPG, please refer to [6]. The detailed steps of ALSPG are outlined in Alg. 1, where \mathcal{P}_{C_i} encompasses both $\mathcal{P}_{\text{VO}_i}$ and $\mathcal{P}_{\mathcal{D}_x}$. After obtaining the optimal control \mathcal{U}_{opt} , we apply the first element to update the robot's state. We then rerun Alg.1 until the robot reaches its destination.

In summarize, through combing GeoPro-VO and ALSPG, the MINLP (8) is converted to a constrained problem like (14), which can greatly improve computational efficiency and obtain real time solution in practice.

Algorithm 1: ALSPG

Input: $\mathbf{x}_0, \mathcal{U}_{\text{init}}, \mathcal{P}: \mathcal{P}_{\text{VO}}, \mathcal{P}_{\mathcal{D}_x}, \mathcal{P}_{\mathcal{D}_u}, \boldsymbol{\lambda}_{C_i} = \mathbf{0},$
 $\rho_{C_i} = 0.1, \beta = 20, k = 0, N_{\text{iter}} = 0, N_{\text{max}},$
 $\varepsilon_{\text{tol}} = 1^{-2}$

```

1 while  $N_{\text{iter}} \leq N_{\text{max}}$  do
2    $\mathcal{U}_{k+1} = \arg \min_{\mathcal{U}_k \in \mathcal{D}_u} \mathcal{L}(\mathcal{U}_k, \boldsymbol{\lambda}^k, \boldsymbol{\rho}^k)$  with SPG ;
3   for  $\mathcal{P}_{C_i}$  do
4      $\boldsymbol{\lambda}_{C_i}^{k+1} = \rho_{C_i}^k (V_{C_i}(\mathcal{U}_{k+1}, \boldsymbol{\lambda}_{C_i}^k, \rho_{C_i}^k) + \frac{\boldsymbol{\lambda}_{C_i}^k}{\rho_{C_i}^k})$  ;
5     if  $V_{C_i}(\mathcal{U}_{k+1}, \boldsymbol{\lambda}_{C_i}^{k+1}, \rho_{C_i}^k) \leq V_{C_i}(\mathcal{U}_k, \boldsymbol{\lambda}_{C_i}^k, \rho_{C_i}^k)$  then
6        $\rho_{C_i}^{k+1} = \rho_{C_i}^k$ ;
7     else
8        $\rho_{C_i}^{k+1} = \beta \rho_{C_i}^k$ ;
9     end
10  end
11  if  $\|V\| \leq \varepsilon_{\text{tol}}$  then
12    break;
13  end
14   $N_{\text{iter}} \leftarrow N_{\text{iter}} + 1$ ;
15 end
Output: Optimal control  $\mathcal{U}_{\text{opt}}$ .

```

IV. NUMERICAL SIMULATIONS

A. Implementation Details

The effectiveness and performance of GeoPro-VO are evaluated through numerical simulations. All simulations are conducted on an Ubuntu Laptop with Intel Core i9-13900HX processor using Python for all computations. The simulation time step Δt is set as 0.05 s. Furthermore, the maximum values for horizontal velocity $v_x^{\text{max}} = -v_x^{\text{min}}$ and

TABLE I: Setup of Simulation Parameters

Notation	Meaning	Value
v_x^{max}	Robot's maximum horizontal velocity	0.4 m/s
v_y^{max}	Robot's maximum vertical velocity	0.4 m/s
a_x^{max}	Robot's maximum horizontal acceleration	1.0 m/s ²
a_y^{max}	Robot's maximum vertical acceleration	1.0 m/s ²
r	Radius of robot	0.1 m
d_s	Safe margin for collision avoidance	0.03 m
ε_{tol}	Termination criterion of ALSPG	1 ⁻²
N_{max}	Maximum number of iterations	20
N	Prediction horizon of NMPC	6
β	Penalty factor of ALSPG	20
Δt	Time step of simulation	0.05 s

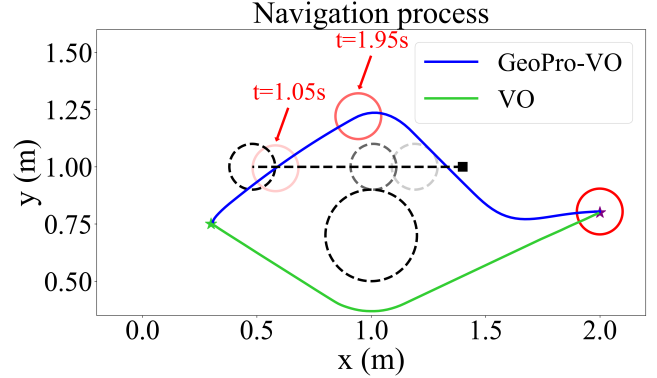


Fig. 4: Robot navigation process

Fig. 5: Simulation results of navigating the robot to its destination while considering both static and dynamic obstacles. The trajectories of our methods (GeoPro-VO) and VO are depicted by blue and green lines, respectively. The starting and ending points of the robot are marked with green and purple stars, respectively. The robot is represented by red circles, while obstacles are shown as black dashed circles. The positions of the robot and dynamic obstacle at various moments are depicted using varying color depth.

acceleration $a_x^{\text{max}} = -a_x^{\text{min}}$, as well as for vertical velocity $v_y^{\text{max}} = -v_y^{\text{min}}$ and acceleration $a_y^{\text{max}} = -a_y^{\text{min}}$, represent the physical limitations of the double integral model (1). To meet safety requirements, we incorporate a safe margin d_s into the radius of robot. The parameters for both the robot dynamics and ALSPG are shown in Tab. I. In the following, we will present simulation results and compare our method with the state of the art.

B. Simulation Results with Static and Dynamic Obstacles

In this section, we mainly demonstrate effectiveness of our method. The prediction horizon of NMPC is set as 6. The robot's initial and final positions are at (0.3 m, 0.75 m) and (2.0 m, 0.8 m), respectively. Moreover, there are two obstacles in the environment: one static obstacle and another dynamic obstacle moved at a velocity $(-0.2 \text{ m/s}, 0.0 \text{ m/s})$. The navigation process of the robot is illustrated in Fig. 5, our method successfully navigate the robot towards its destination while avoiding collisions with all obstacles, where the trajectory of our method is depicted in blue, while the

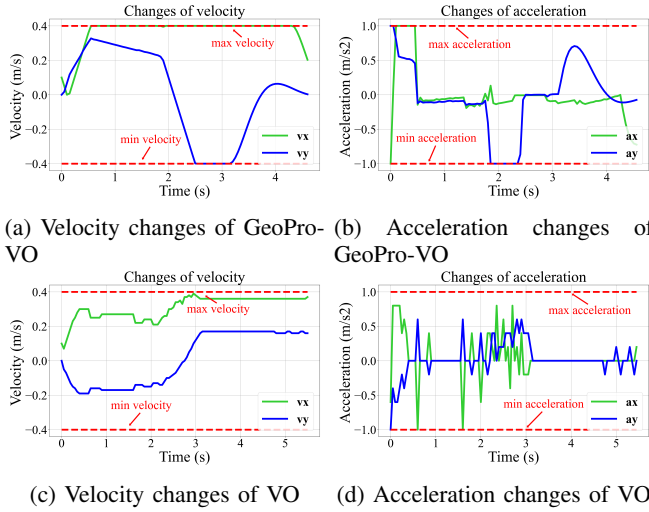


Fig. 6: Velocity and acceleration changes of our method GeoPro-VO and VO.

trajectory of the nominal VO [13] is shown in green, and the dynamic obstacle's path is represented by a black dashed line. The nominal VO method does not utilize the constrained NMPC framework, hence it tends to avoid obstacles from below for safety requirements. In contrast, our approach opts to evade obstacles on the same side as it also accounts for safety constraints within the prediction horizon. In addition, when reducing N to 2, our method also chooses to avoid obstacles from below. The positions of both the robot and dynamic obstacle at different time moments are indicated by varying colors' depths.

The velocity and acceleration change curves for both our method and the nominal VO are shown in Fig. 6, illustrating the changes during the navigation process. It is evident that both approaches adhere to the physical limitations of states and controls. However, since the nominal VO is designed for collision avoidance in the velocity space, it is unsuitable for a robot controlled by acceleration. This can lead to unstable behavior of acceleration, as illustrated in Fig. 6d. On the contrary, our method manipulates in the acceleration space, resulting in smoother curves, as shown in Fig. 6b.

C. Efficient Computation of ALSPG

In this section, we mainly demonstrate the advantage for computation speed of ALSPG through comparing it with the commercial second-order solvers. All optimization problems are formulated as constrained NMPC and solved using various solvers. For constrained NMPC using VO as obstacle avoidance constraints, the nominal optimization problem (8) is solved by BONMIN [19], which is a solver designed for MINLP. Similarly, for constrained NMPC using Euclidean distance as obstacle avoidance constraints, the nominal optimization problem (2) is solved by IPOPT [20]. Furthermore, the constrained NMPC problems with two different types of constraints mentioned above can also be solved using ALSPG with the help of GeoPro. The maximum computation time of ALSPG will occur in the first few runs of it because

TABLE II: Comparison of Different Types of Constraints in Optimization Problems

Constraint Types ^a	Solver	Scenario	Time (ms)			
			Max	Min	Median	Avg
Velocity Obstacle based Constraints	ALSPG ^b N=2	S2 ^e	80.69	2.86	3.12	14.29
		S4	200.57	5.08	49.42	40.72
		D1 ^f	84.08	1.17	1.76	8.39
		D2	113.49	2.83	3.05	10.97
		D3	121.56	3.99	8.78	16.77
		S2	126.01	4.28	89.41	70.51
	ALSPG N=6	S4	765.52	10.22	207.38	236.48
		D1	130.29	3.30	52.81	57.46
		D2	435.53	4.43	86.49	117.23
		D3	608.40	6.31	140.91	157.28
		S2	2189.86	63.64	88.28	287.81
		S4	157842	111.18	141.24	9273.05
	BONMIN ^c N=6	D1	856.92	43.33	63.69	114.27
		D2	3137.72	63.53	98.91	377.28
		D3	4440.58	85.46	160.23	947.50
Euclidean Distance based Constraints	ALSPG N=2	S2	15.15	0.97	1.08	2.92
		S4	20.54	1.36	1.48	3.96
		D1	N/A	N/A	N/A	N/A
		D2	N/A	N/A	N/A	N/A
		D3	N/A	N/A	N/A	N/A
		S2	37.15	1.19	25.75	20.15
	ALSPG N=6	S4	51.81	1.77	37.26	29.27
		D1	36.84	1.15	17.55	16.46
		D2	N/A	N/A	N/A	N/A
		D3	N/A	N/A	N/A	N/A
		S2	301.15	12.77	16.28	21.23
	IPOPT ^d N=6	S4	301.44	19.24	22.81	28.33
		D1	291.73	10.98	14.73	24.15
		D2	N/A	N/A	N/A	N/A
		D3	N/A	N/A	N/A	N/A

^a All optimization setup are formulated as constrained NMPC problems.

^b ALSPG is used in conjunction with the geometric projector.

^c BONMIN is a solver for the mixed integer nonlinear programming problem.

^d IPOPT is a solver for the nonlinear optimization problem.

^e S2 means one robot and two static obstacles.

^f D1 means one robot and one dynamic obstacle.

it requires more iterations to converge to assure that all constraints are satisfied. To reduce the computation time, we can use the final result from the previous optimization round as the initial value for the next round. This trick is also applicable to the commercial solvers.

The comparison results are shown in Tab. II, where five scenarios are considered: S2: a robot with two static obstacles; S4: a robot with four static obstacles; D1: a robot with one dynamic obstacle; D2: a robot with two dynamic obstacles; D3: a robot with three dynamic obstacles. We can observe that although IPOPT is implemented in C++, ALSPG (implemented in Python) has similar calculation speeds as it. The increased efficiency is attributed to GeoPro's capability to handle non-smooth safe constraints like (4), as well as ALSPG only requires the first-order information of the objective function. When comparing ALSPG to BONMIN, we can observe ALSPG also demonstrates greater computational efficiency. The large computation time of VO-NMPC (8) solved by BONMIN arises from it adds integer variables to the optimization problem (8) to cope with the problem that at least one of two constraints (7) needs to be satisfied, transforming the nominal problem (2) into a MINLP (8).

D. Reliable Security of GeoPro-VO

When comparing these two geometric projectors GeoPro-VO and GeoPro-ED, our method GeoPro-VO requires more computation time under the same prediction horizon, as shown in cases S2 and S4 in Tab. II. This is due to GeoPro-

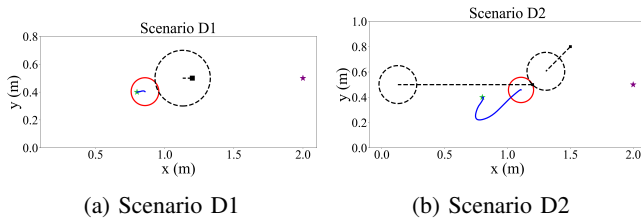


Fig. 7: Failure scenarios when using ALSPG with GeoPro-ED for dynamic obstacle avoidance. (a): The prediction horizon of NMPC is set as 2. (b): The prediction horizon of NMPC is set as 6.

VO involves additional complex calculations for constructing the GeoPro, such as constructing hyperplanes and projecting the unsafe velocity onto the nearest hyperplane. In contrast, GeoPro-ED involves fewer calculations with lower computational complexity, as shown in (5). When analyzing scenarios with dynamic obstacles, we can observe that ALSPG with GeoPro-ED in the case of prediction horizon of 2 fails to achieve collision avoidance with the dynamic obstacle in scenario D1, as shown in Fig. 7a. Moreover, for the other two scenarios D2 and D3, ALSPG with GeoPro-ED also fails to avoid collisions with dynamic obstacles even with prediction horizon of 6, the details of scenario D2 is shown in Fig. 7b. In contrast, ALSPG with our method GeoPro-VO successfully avoids collisions with all dynamic obstacles even the MPC prediction horizon is set at 2. This difference arises from VO's ability to anticipate and avoid collisions in the velocity space, whereas GeoPro-ED focuses on collision avoidance in the position space. In addition, since GeoPro-VO has the ability of assuring safety even with a short prediction of MPC, we can reduce the prediction horizon of MPC when solving through ALSPG with GeoPro-VO to improve solution efficiency.

In conclusion, solving VO-NMPC using ALSPG with GeoPro-VO is more computationally efficient than solved by BONMIN. In comparison to GeoPro-ED, GeoPro-VO requires more time for computation due to the complexity involved in constructing the GeoPro. However, GeoPro-VO performs well in ensuring safety with dynamic obstacles when solving the constrained NMPC problem with a short prediction horizon through ALSPG, while GeoPro-ED falls short in this aspect.

V. CONCLUSIONS

In this paper, we propose a geometric projector for dynamic obstacle avoidance based on velocity obstacle (GeoPro-VO). Furthermore, we integrate GeoPro-VO with the augmented Lagrangian spectral projected gradient descent (ALSPG) algorithm to reformulate the nominal constrained nonlinear model predictive control (NMPC) problem as a sub-optimization problem and solve it efficiently. The effectiveness and performance of our method is validated through numerical simulations, and results demonstrate that our method successfully guides the robot to its destination without any collisions with both static and dynamic

obstacles. Compared to the state of the art, our method is more computationally efficient and can ensure safety with dynamic obstacles even with a short prediction horizon of NMPC. Future research will focus on improving the computational efficiency of our method and extending it to multi-robot systems.

REFERENCES

- [1] Z. Wang, X. Zhou, C. Xu, and F. Gao, "Geometrically constrained trajectory optimization for multicopters," *IEEE Transactions on Robotics*, vol. 38, no. 5, pp. 3259–3278, 2022.
- [2] Y. Wang, Y. Liu, M. Leibold, M. Buss, and J. Lee, "Hierarchical incremental mpc for redundant robots: a robust and singularity-free approach," *IEEE Transactions on Robotics*, 2024.
- [3] G. Torrisi, S. Grammatico, R. S. Smith, and M. Morari, "A projected gradient and constraint linearization method for nonlinear model predictive control," *SIAM Journal on Control and Optimization*, vol. 56, no. 3, pp. 1968–1999, 2018.
- [4] P. E. Gill, W. Murray, and M. A. Saunders, "Snopt: An sqp algorithm for large-scale constrained optimization," *SIAM review*, vol. 47, no. 1, pp. 99–131, 2005.
- [5] E. G. Birgin, J. Martínez, and M. Raydan, "Spectral projected gradient methods," *Encyclopedia of Optimization*, vol. 2, 2009.
- [6] E. G. Birgin, J. M. Martínez, and M. Raydan, "Spectral projected gradient methods: review and perspectives," *Journal of Statistical Software*, vol. 60, pp. 1–21, 2014.
- [7] R. Andreani, E. G. Birgin, J. M. Martínez, and M. L. Schuverdt, "On augmented lagrangian methods with general lower-level constraints," *SIAM Journal on Optimization*, vol. 18, no. 4, pp. 1286–1309, 2008.
- [8] E. G. Birgin and J. M. Martínez, *Practical augmented Lagrangian methods for constrained optimization*. SIAM, 2014.
- [9] X. Jia, C. Kanzow, P. Mehlitz, and G. Wachsmuth, "An augmented lagrangian method for optimization problems with structured geometric constraints," *Mathematical Programming*, vol. 199, no. 1-2, pp. 1365–1415, 2023.
- [10] H. Girgin, T. Löw, T. Xue, and S. Calinon, "Projection-based first-order constrained optimization solver for robotics," *arXiv preprint arXiv:2306.17611*, 2023.
- [11] X. Chi, T. Löw, Y. Li, Z. Liu, and S. Calinon, "Geometric projectors: Geometric constraints based optimization for robot behaviors," *arXiv preprint arXiv:2309.08802*, 2023.
- [12] A. Chakravarthy and D. Ghose, "Obstacle avoidance in a dynamic environment: a collision cone approach," *IEEE Transactions on Systems, Man, and Cybernetics - Part A: Systems and Humans*, vol. 28, no. 5, pp. 562–574, 1998.
- [13] P. Fiorini and Z. Shiller, "Motion planning in dynamic environments using velocity obstacles," *The international journal of robotics research*, vol. 17, no. 7, pp. 760–772, 1998.
- [14] J. van den Berg, M. Lin, and D. Manocha, "Reciprocal velocity obstacles for real-time multi-agent navigation," in *2008 IEEE International Conference on Robotics and Automation*, 2008, pp. 1928–1935.
- [15] J. v. d. Berg, S. J. Guy, M. Lin, and D. Manocha, "Reciprocal n-body collision avoidance," in *Robotics research*. Springer Berlin Heidelberg, 2011, pp. 3–19.
- [16] J. Snape, J. v. d. Berg, S. J. Guy, and D. Manocha, "The hybrid reciprocal velocity obstacle," *IEEE Transactions on Robotics*, vol. 27, no. 4, pp. 696–706, 2011.
- [17] H. Cheng, Q. Zhu, Z. Liu, T. Xu, and L. Lin, "Decentralized navigation of multiple agents based on orca and model predictive control," in *2017 IEEE/RSJ International Conference on Intelligent Robots and Systems (IROS)*, 2017, pp. 3446–3451.
- [18] X. Zhang, J. Ma, Z. Cheng, M. Tomizuka, and T. H. Lee, "Velocity obstacle based risk-bounded motion planning for stochastic multi-agent systems," *arXiv preprint arXiv:2202.09748*, 2022.
- [19] S. Sutradhar, N. D. Choudhury, and N. Sinha, "Minlp for hydro-thermal unit commitment problem using bonmin solver," in *2016 IEEE 1st International Conference on Power Electronics, Intelligent Control and Energy Systems (ICPEICES)*, 2016, pp. 1–6.
- [20] L. Biegler and V. Zavala, "Large-scale nonlinear programming using ipopt: An integrating framework for enterprise-wide dynamic optimization," *Computers & Chemical Engineering*, vol. 33, no. 3, pp. 575–582, 2009.